

## 02 Spectroscopic study of $\text{KY}_3\text{F}_{10}$ crystals doped with praseodymium

© E.P. Chukalina,<sup>1</sup> T.A. Igolkina,<sup>1,2</sup> D.N. Karimov<sup>3</sup>

<sup>1</sup> Institute of Spectroscopy of RAS, 108840 Troitsk, Moscow, Russia

<sup>2</sup> Moscow Institute of Physics and Technology (National Research University), 141700 Dolgoprudny, Moscow Region, Russia

<sup>3</sup> Shubnikov Institute of Crystallography of FSRC „Crystallography and Photonics“ RAS, 119333 Moscow, Russia

e-mail: echukalina@isan.troitsk.ru

Received July 22, 2021

Revised July 22, 2021

Accepted August 07, 2021

We report on the high-resolution Fourier spectroscopy study of  $\text{KY}_3\text{F}_{10}:\text{Pr}^{3+}$  crystals. The analysis of the transmission and luminescence spectra allowed us to refine and supplement the information on the crystal-field levels of the  $\text{Pr}^{3+}$  ion. The value of the hyperfine splitting of the ground state of  $\text{Pr}^{3+}$  in the  $\text{KY}_3\text{F}_{10}$  cubic host is estimated. The observed shape of the spectral lines indicates the presence of defects in the sample under study.

**Keywords:**  $\text{KY}_3\text{F}_{10}:\text{Pr}^{3+}$  crystal, Fourier spectroscopy, transmission and luminescence spectra.

DOI: 10.21883/EOS.2022.01.52989.25-21

### Introduction

Crystals of complex fluorides  $\text{KY}_3\text{F}_{10}$  are transparent in a wide range of the spectrum, thermally and chemically stable and isotropic. Doping with rare-earth (RE) ions provides the possibility of their application as laser media and white light emitters. In particular, cw laser radiation was obtained in green (554 nm) [1], orange (610 nm) [2], red (644.5 nm, 720 nm) [3,4] regions of the spectrum. In addition, on  $\text{Pr}:\text{KY}_3\text{F}_{10}$  crystals a quasi-continuous laser with frequency tuning in several intervals between 521 nm and 737 nm with a total tuning range exceeding 100 nm was developed [1].

The paper [5] reported about the study of the optical and scintillation properties of  $\text{KY}_3\text{F}_{10}$  single crystals doped with  $\text{Pr}^{3+}$  ions. When excited by radiation with a wavelength of 210 nm, an intense photoluminescence was observed at wavelength of 300 nm, corresponding to  $5d-4f$  transition in the  $\text{Pr}^{3+}$  ion. The decay time of scintillations in the  $\text{KY}_3\text{F}_{10}:\text{Pr}^{3+}$  crystal for activator concentrations of 1 and 5 at% was 4.5 and 2.5 ns, and the scintillation light output is 700 and 300 photons/5.5 MeV- $\alpha$ , respectively. The results obtained allow us to consider  $\text{KY}_3\text{F}_{10}:\text{Pr}^{3+}$  single crystals as promising for application in  $\gamma$ -radiation detectors.

The use of  $\text{KY}_3\text{F}_{10}$  crystals doped with ions of rare-earth (RE) elements as laser media presupposes both the availability of proven technologies for growing large crystals of the required optical quality and knowledge of the energy scheme of Stark levels of the RE ion. There are certain difficulties in growing  $\text{KY}_3\text{F}_{10}$  crystals of high optical quality, even using well proven melt methods of crystallization. As compared to other fluoride compounds, crystals  $\text{KR}_3\text{F}_{10}$  ( $R = \text{Y}$ , RE element) are more susceptible to pyrohydrolysis and often grow cloudy and opalescent due to high content of oxygen

impurities [6]. The quality control of the grown crystals is possible using the high-resolution spectroscopy method. In particular, the study of the shape features of spectral lines related to  $f-f$ -transitions in the  $\text{R}^{3+}$  ion can answer the question of the defects presence in the crystal.

The only spectroscopic study of  $\text{KY}_3\text{F}_{10}:\text{Pr}^{3+}$  crystals in the region of  $f-f$ -transitions in the  $\text{Pr}^{3+}$  ion was carried out in the paper [7], where based on analysis of the transmission and luminescence spectra, registered with resolution  $0.25 \text{ cm}^{-1}$ , 39 Stark levels of the  $\text{Pr}^{3+}$  ion were determined, and calculation was made according to the theory of the crystal field (CF). However, out of seven levels of the ground multiplet  $^3\text{H}_4$  of the  $\text{Pr}^{3+}$  ion only five levels were determined, and there is no information about the levels of  $^1\text{G}_4$  multiplet. In this paper, the results of a spectroscopic study with high spectral resolution of crystals  $\text{KY}_3\text{F}_{10}:\text{Pr}^{3+}$  (0.01 at%) were presented, they ensure significant clarification and supplement of data in paper [7].

### Information about structure

Under normal conditions the  $\text{KY}_3\text{F}_{10}$  crystal has a cubic structure with the space group of symmetry  $Fm-3m$  [8]. This structure is shown schematically in Fig. 1. It can be represented as ionic groups  $[\text{KY}_3\text{F}_8]^{2+}$  and  $[\text{KY}_3\text{F}_{12}]^{2-}$  alternating along three crystallographic directions. Trivalent RE ions replace  $\text{Y}^{3+}$  ions and occupy position with tetragonal symmetry (point group of symmetry  $C_{4v}$ ). The closest environment of the RE ion in  $\text{KY}_3\text{F}_{10}$  is 8  $\text{F}^-$  ions forming a square antiprism with different base sizes. Thus, equivalent RE optical centers are formed in this crystal, they are oriented along three different axes  $C_4$  of the face-centered cubic lattice.

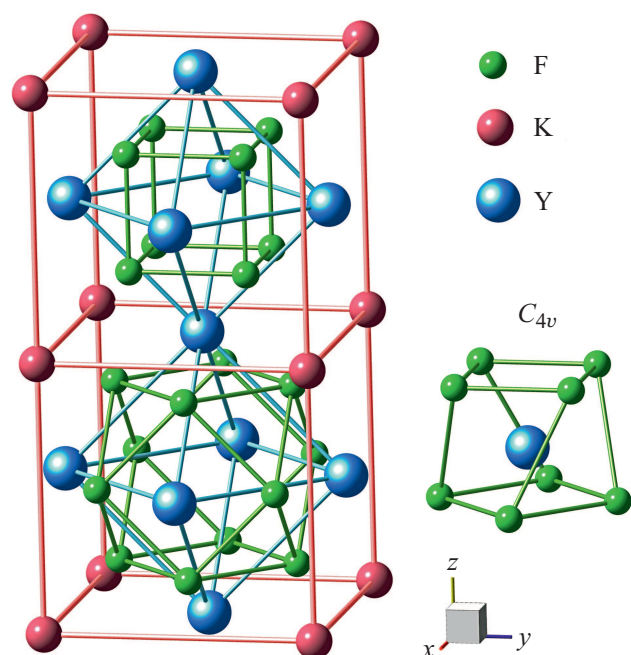


Figure 1. Crystal structure of  $KY_3F_{10}$ .

## Experiment

$KY_3F_{10}:Pr^{3+}$  (0.01 at%) single crystals were grown by the Bridgman–Stockbarger method in  $CF_4$  atmosphere in graphite crucibles from a melt of stoichiometric composition. Anhydrous powders  $YF_3$  and  $PrF_3$  (99.99, LANHIT Ltd.), and  $KHF_2$  hydrofluoride were used as initial reagents, the later was obtained by the reaction of carbonate  $K_2CO_3$  (99.995, Sigma-Aldrich) with concentrated HF solution, were used. The growth was carried out at a temperature of 1350 K with a pulling rate of 3 mm/h. Details of the growth experiment are given in [8]. Transparent crystals with perfect cleavage along planes (111) were obtained (Fig. 2). According to data of X-ray phase analysis (Rigaku MiniFlex 600 X-ray diffractometer,  $CuK\alpha$  radiation),  $KY_3F_{10}:Pr$  crystals were single-phase and had cubic symmetry (space group  $Fm\bar{3}m$ ) with lattice parameter  $a = 1.1547$  nm. The sample 11.2 mm thick was prepared for measurements.

The transmission and luminescence spectra of crystals  $KY_3F_{10}:Pr^{3+}$  (0.01 at%) were recorded with a resolution of up to  $0.01\text{ cm}^{-1}$  in a wide spectral range from 2000 to  $22000\text{ cm}^{-1}$  and temperature range from 5 to 300 K on a Bruker IFS 125HR high-resolution Fourier spectrometer. The sample was placed in a Cryomech ST403 closed cycle optical cryostat. The luminescence of the sample was excited by cw semiconductor laser with a radiation wavelength of  $\lambda = 462$  nm. The laser radiation power density was  $50\text{ mW/mm}^2$ .

## Results and discussion

$Pr^{3+}$  ion has two electrons in the  $4f$  shell. The electronic configuration  $4f^2$  in a centrally symmetric field gives 7 terms, which are split into 13 SLJ multiplets due to the spin-orbit interaction: four singlet and nine triplet multiplets. The ground level is  $^3H_4$ . Bands of absorption by  $Pr^{3+}$  ions due to  $^3H_4 \rightarrow ^3H_{5,6}$ ,  $^3F_{2,3,4}$  transitions are in the mid-infrared region; transitions to levels  $^1G_4$  and  $^1D_2$  are spin-forbidden (in the spectra they appear due to admixture of other states); transitions to the level  $^3P_0$  occur due to the absorption of radiation quanta in the visible range. In a crystal field  $KY_3F_{10}$  the energy levels of free ion  $Pr^{3+}$  are split into Stark sublevels, whose wave functions are transformed according to non-degenerate irreducible representations  $\Gamma_1, \Gamma_2, \Gamma_3, \Gamma_4$  and the doubly degenerate  $\Gamma_5$  of point group of symmetry  $C_{4v}$ . The number and symmetry of Stark levels for multiplets with a total moment  $J$  from 0 to 6 for the ion with an even number of electrons (as in the case of  $Pr^{3+}$ ) in positions with the point group of symmetry  $C_{4v}$  are given in Table 1. Table 2 lists the selection rules for electric dipole (ED) and magnetic dipole (MD) transitions in the case of the point group of symmetry  $C_{4v}$ . Since there are equivalent RE centers oriented along three different axes  $C_4$  of the cubic lattice, there is no polarization dependence in the spectra. Note, however, that  $\Gamma_{3,4} \leftrightarrow \Gamma_{1,2}$  optical transitions are strictly forbidden; transitions involving  $\Gamma_5$  levels are allowed as both ED and MD; transitions  $\Gamma_k \rightarrow \Gamma_k$  ( $k = 1, 2, 3, 4$ ) are carried out as ED, only, and transitions  $\Gamma_1 \leftrightarrow \Gamma_2$  and  $\Gamma_3 \leftrightarrow \Gamma_4$  are allowed as MD, only.

Figure 3 shows the low-temperature transmission and luminescence spectra of the crystal  $KY_3F_{10}:Pr^{3+}$  (0.01 at%). The observed transitions are indicated in the diagram on the right. Figure 4, *a–d* shows the transmission spectra at temperature close to that of liquid helium in the region of transitions  $^3H_4 \rightarrow ^3H_5, ^3H_6, ^3F_4, ^1G_4$ . These spectra reflect the structure of excited multiplets, due to the fact that the first excited state of the ground multiplet, according to [7],

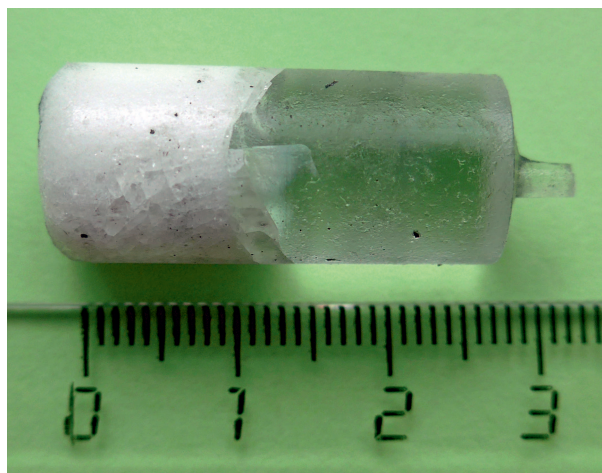
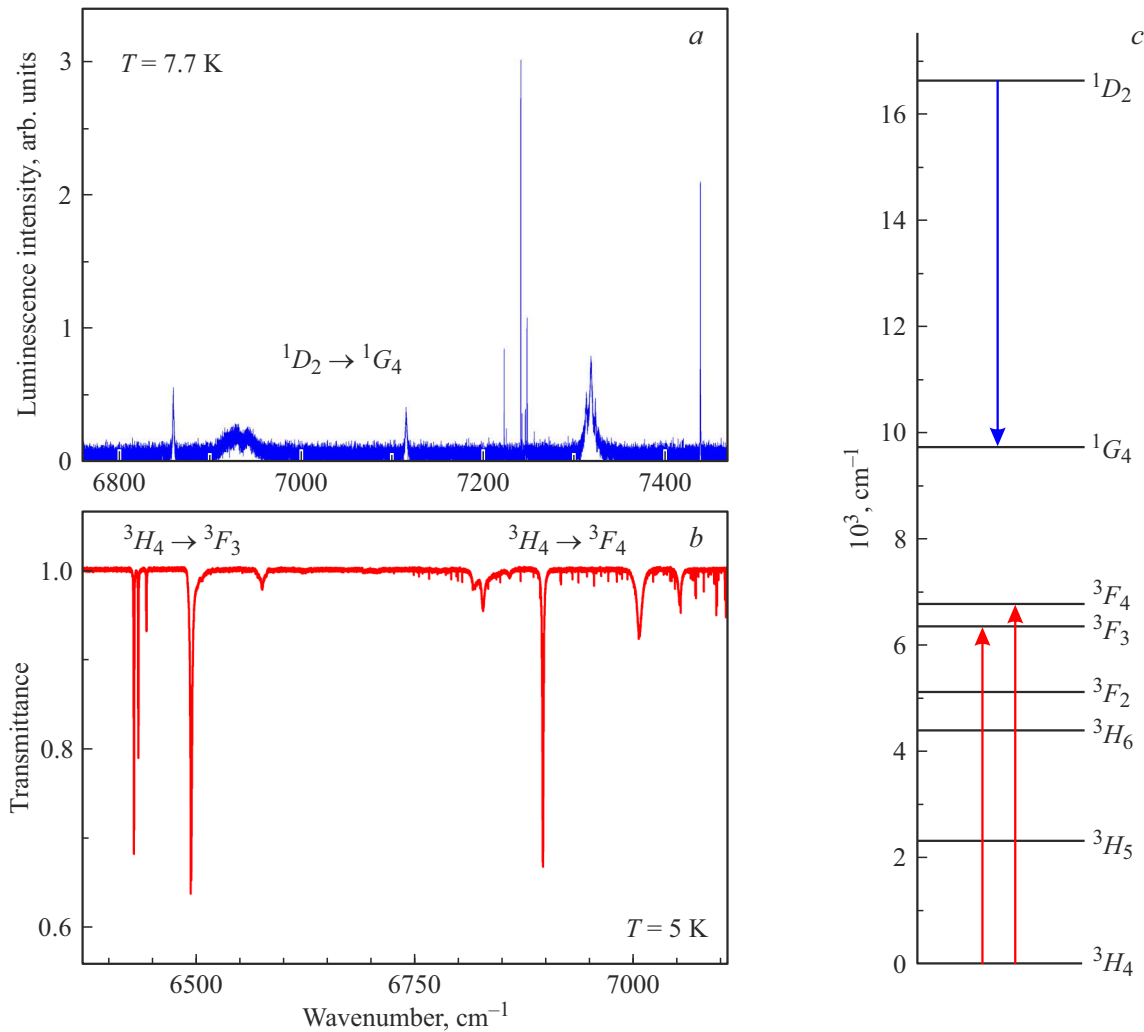


Figure 2. Grown single crystal  $KY_3F_{10}:Pr^{3+}$  (0.01 at%).



**Figure 3.** Luminescence (a) and transmission (b) spectra of the crystal  $KY_3F_{10}:Pr^{3+}$  (0.01 at%). The observed transitions are indicated in the diagram on the right (c).

**Table 1.** The number of Stark levels and their symmetry for a multiplet with a common momentum  $J$  of a non-Kramers rare-earth ion in a crystal field of symmetry  $C_{4v}$

J	Number of levels	Irreducible representations
0	1	$\Gamma_1$
1	2	$\Gamma_2 + \Gamma_5$
2	4	$\Gamma_1 + \Gamma_3 + \Gamma_4 + \Gamma_5$
3	5	$\Gamma_2 + \Gamma_3 + \Gamma_4 + 2\Gamma_5$
4	7	$2\Gamma_1 + \Gamma_2 + \Gamma_3 + \Gamma_4 + 2\Gamma_5$
5	8	$\Gamma_1 + 2\Gamma_2 + \Gamma_3 + \Gamma_4 + 3\Gamma_5$
6	10	$2\Gamma_1 + \Gamma_2 + 2\Gamma_3 + 2\Gamma_4 + 3\Gamma_5$

has an energy exceeding  $100\text{ cm}^{-1}$  and is not populated. The designations of the lines are given in accordance with

the diagram in Fig. 5: Arabic numerals enumerate the Stark levels of the ground multiplet, and capital Latin letters are for the levels of excited multiplets. Recall that the article [7] has no data on the Stark structure of  $^1G_4$  multiplet levels. From the analysis of our absorption and luminescence spectra, we determined the energies of five of the seven Stark levels of  $^1G_4$  multiplet.

As the temperature increases, spectral lines appear in the transmission spectra, these lines correspond to transitions from the excited levels of the ground multiplet  $^3H_4$ . Figure 6 shows the temperature dependence of the spectra in the region of transitions  $^3H_4 \rightarrow ^3F_2, ^3F_3$ . Figure 6, a, b shows the marked transitions from the excited levels of the ground multiplet  $^3H_4$ : 2A, 2B, 2C, 4A, 4C and 5A. Frequency differences of lines 2A, 4A, and 5A and line 1A in the region of transition  $^3H_4 \rightarrow ^3F_2$  (Fig. 6, a) correspond to the energies of the Stark levels 2, 4, and 5 of the ground multiplet  $^3H_4$  of the  $Pr^{3+}$  ion, respectively. The energy of level 2 is confirmed by the position of the line 2A in the region of transition  $^3H_4 \rightarrow ^3F_3$  (Fig. 6, b). Note that the

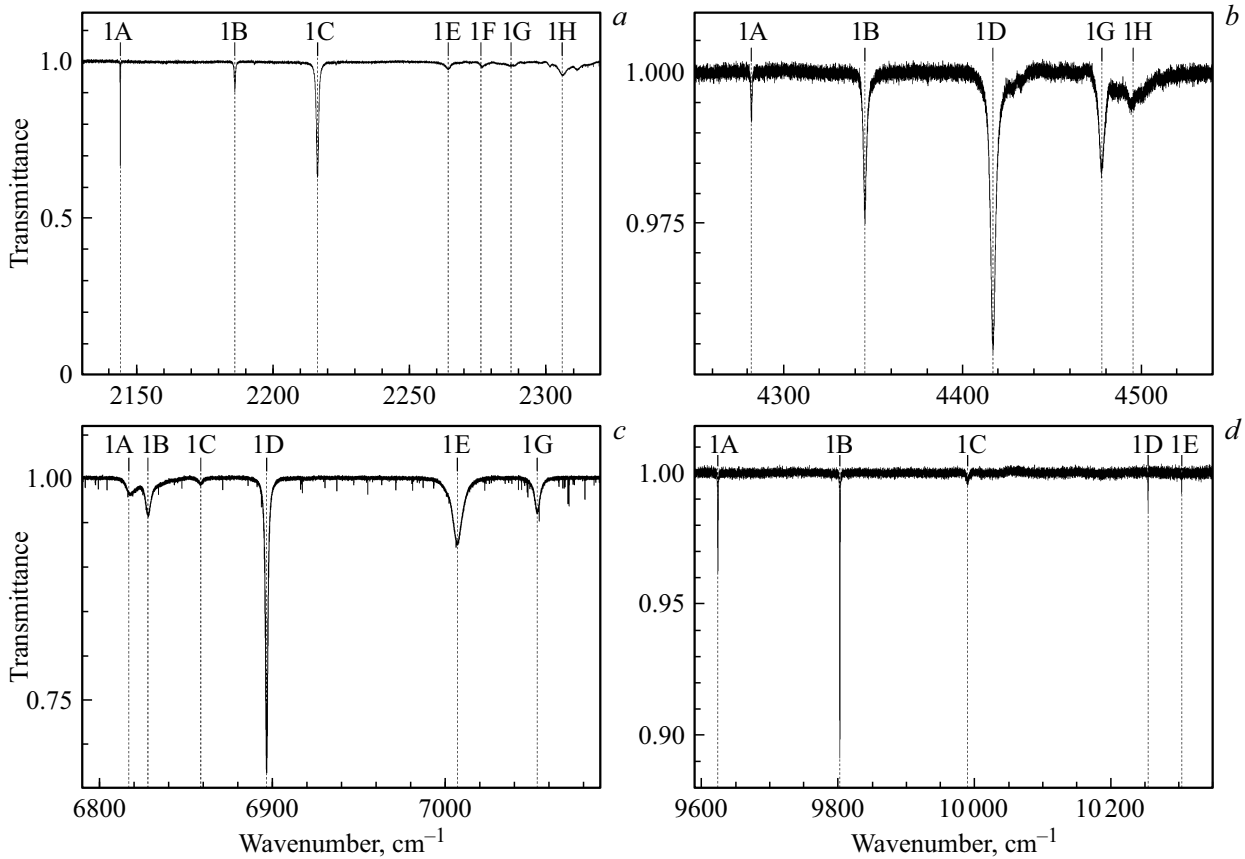


**Figure 4.** Transmission spectrum in the region of transitions:  ${}^3\text{H}_4 \rightarrow {}^3\text{H}_5$  (a),  ${}^3\text{H}_4 \rightarrow {}^3\text{H}_6$  (b),  ${}^3\text{H}_4 \rightarrow {}^3\text{F}_4$  (c),  ${}^3\text{H}_4 \rightarrow {}^1\text{G}_4$  (d) in the  $\text{Pr}^{3+}$  ion in the crystal  $\text{KY}_3\text{F}_{10}:\text{Pr}^{3+}$  (0.01 at%) at temperature 5 K. The designations of the spectral lines are given in accordance with the diagram in Fig. 5.

**Table 2.** Selection rules for electric dipole ( $d_{x,y,z}$ ) and magnetic dipole ( $\mu_{x,y,z}$ ) transitions in the case of the point group of symmetry  $C_{4v}$ . Here,  $x, y, z$  are the local axes of the center of symmetry  $C_{4v}$ . In a cubic crystal  $\text{KY}_3\text{F}_{10}$  the local axis  $z$  is oriented along one of the three equivalent axes  $C_4$  of the cube

$\Gamma_i$	$\Gamma_1$	$\Gamma_2$	$\Gamma_3$	$\Gamma_4$	$\Gamma_5$
$\Gamma_1$	$d_z$	$\mu_z$	—	—	$\mu_{x,y}, d_{x,y}$
$\Gamma_2$	$\mu_z$	$d_z$	—	—	$\mu_{x,y}, d_{x,y}$
$\Gamma_3$	—	—	$d_z$	$\mu_z$	$\mu_{x,y}, d_{x,y}$
$\Gamma_4$	—	—	$\mu_z$	$d_z$	$\mu_{x,y}, d_{x,y}$
$\Gamma_5$	$\mu_{x,y}, d_{x,y}$	$\mu_{x,y}, d_{x,y}$	$\mu_{x,y}, d_{x,y}$	$\mu_{x,y}, d_{x,y}$	$d_z, \mu_z$

level 2 energy of  ${}^3\text{H}_4$  multiplet is determined in our paper for the first time. Also, the energies of levels 4 and 5 of  ${}^3\text{H}_4$  multiplet were refined in comparison with the data of [7].

Thus, the analysis of the temperature dependence of the transmission spectra in the studied spectral region made it possible to determine the exact energies of the Stark

levels of the excited multiplets  ${}^3\text{H}_{5,6}$ ,  ${}^3\text{F}_{2,3,4}$ ,  ${}^1\text{D}_2$ ,  ${}^1\text{G}_4$  and  ${}^3\text{P}_0$ , and some levels of the ground multiplet  ${}^3\text{H}_4$  of the  $\text{Pr}^{3+}$  ion in  $\text{KY}_3\text{F}_{10}:\text{Pr}^{3+}$ . The spectroscopic data are summarized in Table 3 in comparison with the data of the paper [7]. According to the selection rules (Table 2), if the ground state is a singlet, the lines corresponding to strictly forbidden transitions will not be visible in the low-temperature absorption spectra for all multiplets. But if the ground state is a  $\Gamma_5$  doublet, then transitions to all Stark levels of the given excited multiplet are allowed. Transmission spectra at  $T = 5$  K show transitions to all levels of multiplets  ${}^3\text{F}_2$  (Fig. 6, a) and  ${}^3\text{F}_3$  (Fig. 6, b). This speaks in favor of the fact that the ground state is  $\Gamma_5$  doublet, which agrees with the calculation by the CF theory presented in the paper [7]. In the transmission spectra at  $T = 5$  K in each of the regions of transitions  ${}^3\text{H}_4 \rightarrow {}^3\text{H}_5$ ,  ${}^3\text{H}_6$ ,  ${}^3\text{F}_4$ ,  ${}^1\text{G}_4$  shown in Figs. 4, a, 4, b, 4, c, 4, d, respectively, not all possible lines are visible, which can be explained by the low probability of some transitions.

The luminescence spectra show no transitions to the excited levels of the ground  ${}^3\text{H}_4$  multiplet. This conclusion was made from the comparison of the absorption and luminescence spectra at different temperatures. From the luminescence spectra, it was possible to refine the position

**Table 3.** Energies  $E$  of the Stark levels of the  $Pr^{3+}$  ion in the  $KY_3F_{10}-Pr^{3+}$  crystal at  $T = 5$  K and designations of levels adopted in this paper. The experimental values of the energies  $E$  at  $T = 10$  K and the theoretically calculated irreducible representations  $\Gamma_i$  from the paper [7] are also provided

$^{2S+1}L_J$	$E, \text{cm}^{-1}$ at $T = 5$ K	Levels	$E, \text{cm}^{-1}$ [7] at $T = 10$ K	$\Gamma_i$ [7]	$^{2S+1}L_J$	$E, \text{cm}^{-1}$ at $T = 5$ K	Levels	$E, \text{cm}^{-1}$ [7] at $T = 10$ K	$\Gamma_i$ [7]
$^3H_4$	0	1	0	$\Gamma_5$	$^3F_2$	5041.1	A	5042	$\Gamma_3$
	88	2	—	$\Gamma_3$		5073.6	B	5075	$\Gamma_4$
	—	3	136	$\Gamma_1$		5098.8	C	5100	$\Gamma_5$
	163	4	170	$\Gamma_5$		5229.6	D	5230	$\Gamma_1$
	211	5	214	$\Gamma_4$	$^3F_3$	6429	A	6430.3	$\Gamma_3$
	—	6	—	$\Gamma_2$		6434.1	B	6435	$\Gamma_5$
	—	7	508	$\Gamma_1$		6443.5	C	6444.6	$\Gamma_4$
$^3H_5$	2144	A			$^3F_4$	6494.5	D	6497	$\Gamma_5$
	2185.9	B	2186	$\Gamma_5$		6575.6	E	6576.6	$\Gamma_2$
	2216.2	C	2216	$\Gamma_4$		6817	A		
	—	D	—	$\Gamma_2$	6828.1	B	6831	$\Gamma_5$	
	2264	E	2263	$\Gamma_1$	6858	C	6859.4	$\Gamma_3$	
	2276	F	2277	$\Gamma_5$	6896.7	D	6901	$\Gamma_4$	
	2287	G	2287	$\Gamma_3$	7006.9	E	7006	$\Gamma_1$	
	2305.7	H	2306.6	$\Gamma_2$	—	F	—	$\Gamma_2$	
	—	I	2636	$\Gamma_5$	7053.1	G	7056	$\Gamma_5$	
$^3H_6$	4282	A	4285	$\Gamma_1$	$^1G_4$	—	H	7126	$\Gamma_1$
	4345.3	B	4347	$\Gamma_5$		9625	A	—	
	—	C	—	$\Gamma_2$		9803.2	B	—	
	4416.7	D	4417.6	$\Gamma_3$		9900	C	—	
	—	E	4429	$\Gamma_5$		10253.5	D	—	
	—	F	4433.4	$\Gamma_1$	10302.6	E	—		
	4477.4	G	4478	$\Gamma_5$	$^1D_2$	16651.8	A	16557	$\Gamma_4$
	4494.8	H	4495	$\Gamma_4$		16706.4	B	16712	$\Gamma_3$
	—	I	—	$\Gamma_3$		16878	C	16886	$\Gamma_1$
	—	J	—	$\Gamma_4$		—	D	17236	$\Gamma_5$
				$^3P_0$		20725.3	A	20733	$\Gamma_1$

of the only Stark level of  $^3P_0$  multiplet (Table 3). Figure 7 shows the luminescence spectra in the region of transitions from the  $^3P_0$  level to the Stark levels of multiplets  $^3F_4$ ,  $^3F_3$  (Fig. 7, *a*) and  $^3H_6$  (Fig. 7, *b*).

Let us consider in detail the spectral region 6320–6380  $\text{cm}^{-1}$  shown in Fig. 8. Attention is drawn to the complex shape of absorption lines 2A, 2B and 2C in the region of transition  $^3H_4 \rightarrow ^3F_3$ : each of these lines has two components. The distances between the components

of the lines 2A, 2B, and 2C are practically the same and equal to  $2.5 \pm 0.1 \text{ cm}^{-1}$ . It should be noted that no other spectral lines with a pronounced doublet structure were found. What could be the reason for the observed splitting of lines 2A, 2B, and 2C? It is natural to assume the existence of two Stark levels close in energy with energies  $\sim 87$  and  $89 \text{ cm}^{-1}$ . According to the theoretical calculation in the paper [7], level 2 has energy from 105 to  $113 \text{ cm}^{-1}$  depending on the calculation method. The energy

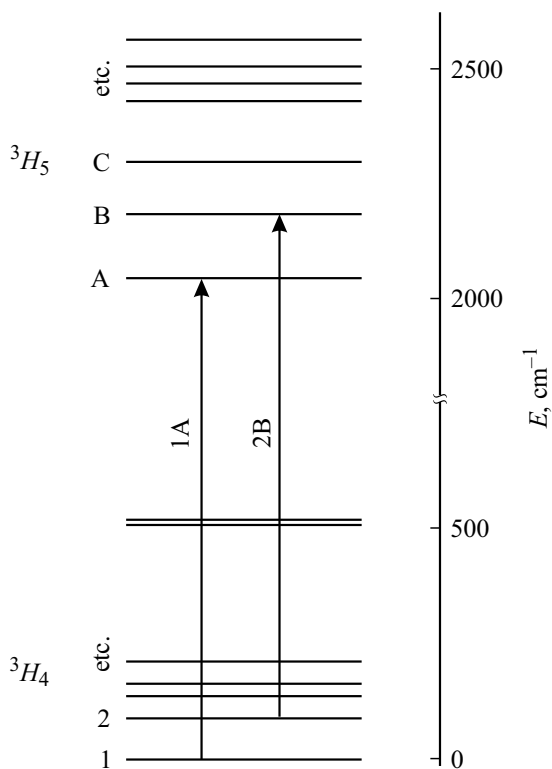


**Figure 5.** Scheme of designations for Stark levels and the corresponding transitions adopted in this work.

of the level 3 was determined experimentally in [7] and is equal to  $136\text{ cm}^{-1}$ , and according to the calculation — from  $121$  to  $133\text{ cm}^{-1}$ . In the spectra of the  $\text{Pr}^{3+}$  ion measured by us in the crystal  $\text{KY}_3\text{F}_{10}:\text{Pr}^{3+}$  (0.01 at%) the spectral lines corresponding to transitions from level 3 of the ground multiplet  $^3\text{H}_4$  are not observed. The energies of levels 4 and 5 were determined (Table 3), and their values are close to the experimental data of the work [7]. Comparison of the spectroscopic data obtained in this paper with the results from the article [7] shows the validity of the theoretical calculation [7], as a result of which the obtained parameters of the crystal field describe mainly the energy structure of the levels of the  $\text{Pr}^{3+}$  ion in the  $\text{KY}_3\text{F}_{10}:\text{Pr}^{3+}$  crystal. However, note that in the case of two excited multiplets  $^3\text{H}_5$  and  $^3\text{F}_4$  the energies of the first Stark levels significantly do not agree with the experimental data of the paper [7], used as the basis of made theoretical calculation (Table 3). The narrow,  $0.07\text{ cm}^{-1}$ , low-frequency line  $2144\text{ cm}^{-1}$  could not be registered in [7] due to the low resolution use. All the above refinements and additions to the energy scheme of the Stark levels of the  $\text{Pr}^{3+}$  ion in the  $\text{KY}_3\text{F}_{10}:\text{Pr}^{3+}$  crystal can lead to correction of the CF parameters obtained earlier in the paper [7].

What other reason exists for this kind of splitting of the considered spectral lines? Random deformations of the crystal lattice caused by various kinds of defects formed during crystal growth can lead to inhomogeneous widening and splitting of spectral lines. The value of the deformation

splitting of the absorption lines varies from a few hundredths to units of a wave number. Splittings similar to those shown in Fig. 8 were observed earlier in the optical spectra of cubic centers of  $\text{Yb}^{3+}$  doping ions in elpasolite crystals [9]. In the paper [9] an explicit expression for the generalized deformations distribution function was obtained, and the splitting of the lines corresponding to optical transitions involving degenerate electronic states was successfully simulated. In our case, the same splitting of three lines 2A, 2B, and 2C indicates the supposed deformation splitting of the Stark level 2 of the ground multiplet  $^3\text{H}_4$  of the  $\text{Pr}^{3+}$  ion. If refer to calculation from paper [7], then the assumption of deformation splitting contradicts the information obtained from calculation of symmetry  $\Gamma_3$  of the first excited state of the ground multiplet  $^3\text{H}_4$  of the  $\text{Pr}^{3+}$  ion in  $\text{KY}_3\text{F}_{10}:\text{Pr}^{3+}$ .

The unresolved hyperfine structure of the spectral lines confirms the assumption about the deformation splittings presence. Figure 9 shows the line  $9625\text{ cm}^{-1}$  in the region of transition  $^3\text{H}_4 \rightarrow ^1\text{G}_4$  in absorption and luminescence spectra. The shape of this line is not described unambiguously by a single contour. Let us estimate the hyperfine splitting of the Stark levels of the  $\text{Pr}^{3+}$  ion in  $\text{KY}_3\text{F}_{10}:\text{Pr}^{3+}$ . The hyperfine structure (HFS) is due to the interaction of the electric and magnetic moments of the nucleus with electrons. Usually, the main contribution to HFS is made by the magnetic dipole hyperfine interaction, which is determined by the magnetic field  $\mathbf{H}(0)$  created on the nucleus by electrons, and by the magnetic moment of the nucleus  $\mu_n$  with spin  $\mathbf{I}$ :

$$V_m = -\mu_n \mathbf{H}(0). \quad (1)$$

In the case of multiplet with given  $\mathbf{J}$ , the Hamiltonian (1) takes the form

$$V_m = A_J(\mathbf{J}\mathbf{I}), \quad (2)$$

where  $A_J$  is the magnetic hyperfine constant. Electron doublets  $\Gamma_5$  split into  $(2I + 1) = 6$  equidistant ultrafine sublevels by magnetic dipole hyperfine interaction. Spin of the praseodymium nucleus is  $^{141}\text{Pr}^{3+}$ :  $I = 5/2$ . In the first approximation, the singlet states do not have HFS. The ground state is doublet  $\Gamma_5$ . This means that all spectral lines in low-temperature absorption spectra must have HFS. The estimate of the  $g$ -factor of the ground state from the parameters of the crystal field calculated in the paper [7] is  $g_z = 4.28$  [10]. Knowing this value, we can calculate the hyperfine splitting  $\Delta E_{\text{HF}}$  of the ground level  $\Gamma_5$  using the formula [11]:

$$\Delta E_{\text{HF}} = A_J \cdot |g_z|/2g_0, \quad (3)$$

where  $A_J$  is magnetic hyperfine constant,  $g_0$  is Lande factor. The magnetic hyperfine constant for the ground multiplet  $^3\text{H}_4$  of the  $\text{Pr}^{3+}$  ion is  $A_J = 1093\text{ MHz} = 0.0364\text{ cm}^{-1}$  [12]. Thus, we obtain an equidistant HFS of levels with an interval between components equal to  $0.0974\text{ cm}^{-1}$ . The calculation according to the crystal field theory using the parameters from the paper [7] made it possible to determine the irreducible

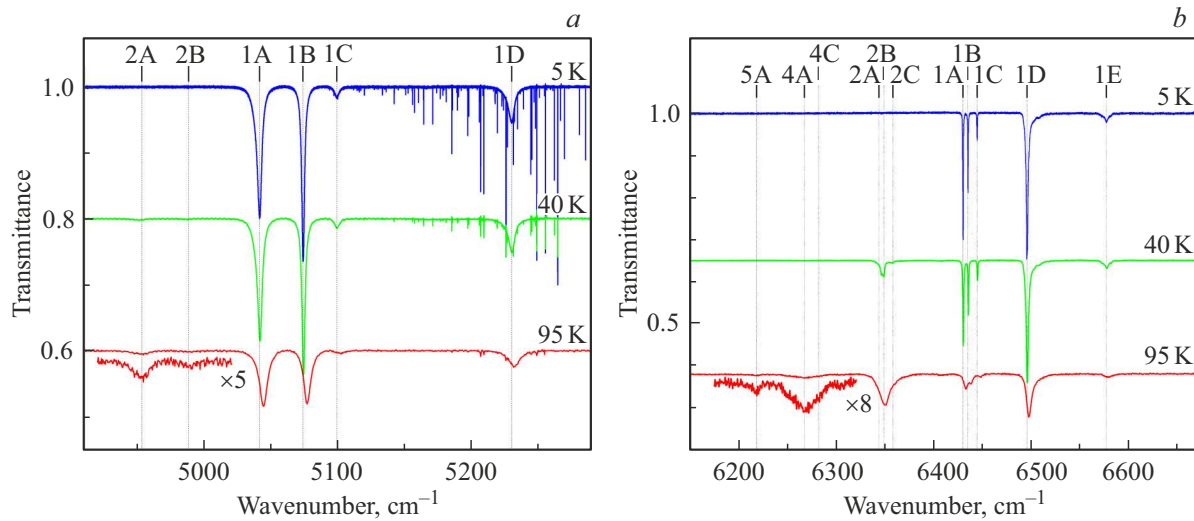


**Figure 6.** Transmission spectrum in the regions of transitions  ${}^3H_4 \rightarrow {}^3F_2$  (a) and  ${}^3H_4 \rightarrow {}^3F_3$  (b) in the  $Pr^{3+}$  ion in the crystal  $KY_3F_{10}:Pr^{3+}$  (0.01 at%) at temperatures 5, 40, 95 K. The designations of the spectral lines are given in accordance with the diagram in Fig. 5. The vertical scale refers to the transmission spectrum at  $T = 5$  K. Narrow lines in the high-frequency region of the spectrum refer to absorption by residual vapors  $H_2O$  in the device.

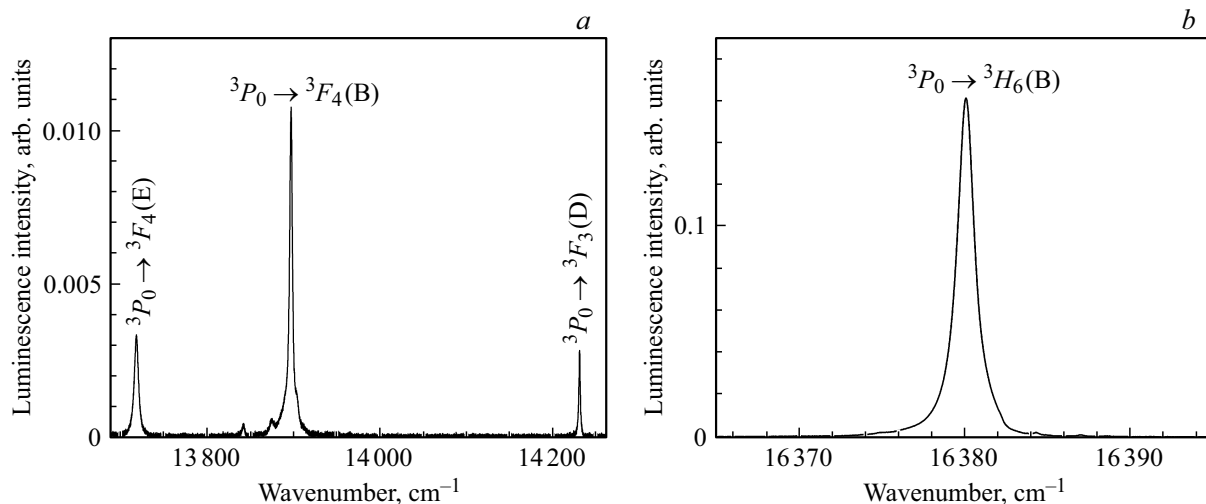


**Figure 7.** Luminescence spectra of the crystal  $KY_3F_{10}:Pr^{3+}$  (0.01 at%) at  $T = 6.6$  K in the region of transitions in the  $Pr^{3+}$  ion from the level  ${}^3P_0$  to Stark levels of multiplets  ${}^3F_4$ ,  ${}^3F_3$  (a) and  ${}^3H_6$  (b). The final level of the transition is indicated in parentheses in the designations given in the diagram in Fig. 5.

representations of the Stark levels of the multiplet  ${}^1G_4$  [10]. According to this calculation, the first level of the excited multiplet  ${}^1G_4$  is a singlet. The half-width of the line  $9625\text{ cm}^{-1}$  is  $0.7\text{ cm}^{-1}$ . Thus, the inhomogeneous widening, probably caused by local changes in the crystal environment of RE ions due to thermal post-growth stresses, did not allow to detect the allowed HFS in the optical spectra of the crystal  $KY_3F_{10}:Pr^{3+}$  (0.01 at%). The observed shape of the line  $9625\text{ cm}^{-1}$  may be due to the combined action of the unresolved HFS and deformation splitting.

As for the doublet structure of the absorption lines 2A, 2B, and 2C in the region of the transition  ${}^3H_4 \rightarrow {}^3F_3$ , then it can be explained by both the presence of two close

levels in the ground multiplet  ${}^3H_4$  and the presence of deformation splitting. Both of these suppositions contradict the calculation according to the theory of the crystal field carried out in the paper [7]. Based on the foregoing, we believe that it is necessary to carry out a new calculation based on the spectroscopic data obtained in this paper.

## Conclusion

The use of high-resolution Fourier spectroscopy made it possible, on the basis of comparative analysis of the temperature dependence of the transmission and luminescence spectra of the  $KY_3F_{10}:Pr^{3+}$  crystal, to significantly

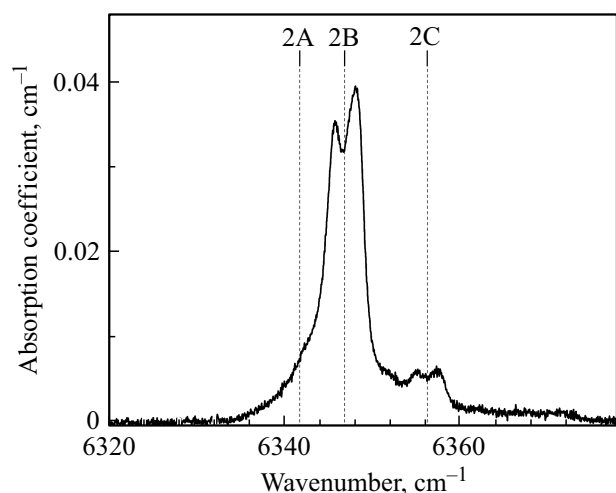


**Figure 8.** Absorption lines 2A, 2B and 2C in the region of transitions  ${}^3H_4 \rightarrow {}^3F_3$  at  $T = 40$  K.

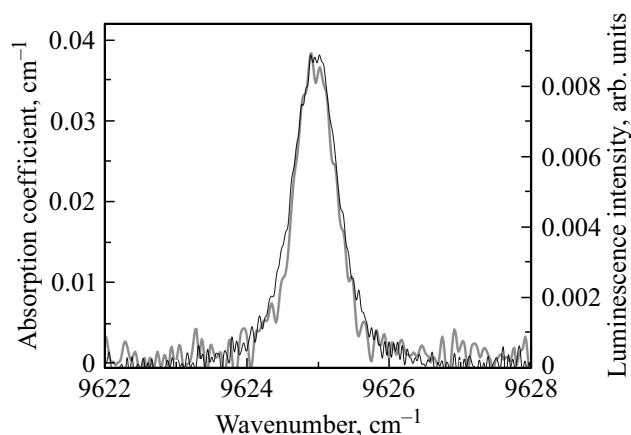


**Figure 9.** The line  $9625\text{ cm}^{-1}$  in the absorption (thin black line) and luminescence (thick gray line) spectra of the crystal  $\text{KY}_3\text{F}_{10}:\text{Pr}^{3+}$  (0.01 at%) at  $T = 5$  K.

refine and supplement the energy diagram of the Stark levels of the  $\text{Pr}^{3+}$  ion. Data on the levels of the excited multiplet  ${}^1G_4$  and the first excited level of the multiplet  ${}^3H_4$  were obtained for the first time. The complex shape of the spectral lines is explained by the combined action of hyperfine and deformation splittings. The splitting of the lines corresponding to the transition from the first excited level of the ground multiplet  ${}^3H_4$  can be explained both by the presence of two close Stark levels and by deformation splitting. The justified decision in favor of one of these two assumptions requires a new calculation according to the crystal field theory based on more complete spectroscopic data obtained in this paper. Besides, to obtain  $\text{KY}_3\text{F}_{10}$  crystals doped with rare-earth ions of the required optical quality, further optimization of the process conditions for their growth from the melt is required.

## Acknowledgments

The work was carried out at the Unique Scientific Unit (USU) of ISAS „Multifunctional high-resolution wide-range spectroscopy“ (USU MHRWRS ISAS), <http://www.ckp-rf.ru/usu/508571>. The authors are grateful to B.Z. Malkin for providing data from the calculation according to the crystal field theory. We express our gratitude to K.N. Boldyrev for his help in recording the luminescence spectra. The authors are grateful to M.N. Popova for valuable comments on the manuscript.

## Funding

The work was financially supported by the Ministry of Science and Higher Education of the Russian Federation, State Assignment № 0039-2019-0004, under the State Assignment theme: „Investigation of new materials, thin films and nanostructures by laser and vibrational spectroscopy and optical microscopy of high and ultrahigh spatial resolution“ № FFUR-2019-0004 and as part of the work under the State Assignment of the Federal Scientific Research Centre „Crystallography and Photonics“ of the Russian Academy of Sciences in the part concerning analysis of crystal properties using the equipment of the Shared Research Center.

## Conflict of interest

The authors declare that they have no conflict of interest.

## References

- [1] P.W. Metz, S. Müller, F. Reichert, D.T. Marzahl, F. Moglia, C. Kränkel, G. Huber. *Optics Express*, **21** (25), 31274 (2013). DOI: 10.1364/OE.21.031274
- [2] B. Xu, P. Camy, J.L. Doualan, Z. Cai, R. Moncorgé. *Optics Express*, **19** (2), 1191 (2011). DOI: 10.1364/OE.19.001191
- [3] P. Camy, J.L. Doualan, R. Moncorgé, J. Bengoechea, U. Weichmann. // *Optics Letters*. 2007. V. 32. № 11. P. 1462. DOI: 10.1364/OL.32.001462
- [4] A. Sottile, P.W. Metz. // *Optics Letters*. 2015. V. 40. № 9. P. 1992. DOI: 10.1364/OL.40.001992
- [5] T. Yanagida, Y. Fujimoto, K. Fukuda. // *Japanese Journal of Applied Physics*. 2014. V. 53. P. 05FK02. DOI: 10.7567/JJAP.53.05FK02
- [6] B. Denker, E. Shklovsky *Handbook of Solid-State Lasers: Materials, Systems and Applications* (Woodhead Publishing Series in Electronic and Optical Materials). Amsterdam: Elsevier, 2013. 688 p.
- [7] J.P.R. Wells, M. Yamaga, T.P.J. Han, H.G. Gallagher. // *J. Physics: Condensed Matter*. 2000. V. 12. № 24. P. 5297. DOI: 10.1088/0953-8984/12/24/318
- [8] D.N. Karimov, I.I. Buchinskaya, N.A. Arkharova, A.G. Ivanova, A.G. Savelyev, N.I. Sorokin, P.A. Popov. // *Crystals*. 2021. V. 11. № 3. 285. DOI: 10.3390/cryst11030285
- [9] B.Z. Malkin, D.S. Pytalev, M.N. Popova, E.I. Baibekov, M.L. Falin, K.I. Gerasimov, N.M. Khaidukov. // *Physical Review B*. 2012. V. 86. P. 134110. DOI: 10.1103/PhysRevB.86.134110

- [10] B.Z. Malkin. Private communication.
- [11] S.A. Klimin, E.P. Chukalina, K.N. Boldyrev, T.A. Igolkina, M.S. Radionov, M.C. Chou, M.N. Popova. // *J. Luminescence*. 2021. V. 235. P. 118003. DOI: 10.1016/j.jlumin.2021.118003
- [12] A. Abragam, B. Bleaney. *Electron paramagnetic resonance of transition ions*. London: Clarendon press, 1970. 700 p.  
A. Abragam, B. Bleaney. *Electron paramagnetic resonance of transition ions*. V. 1. M.: Mir, 1972. 651 p. (in Russian).